HHS Public Access

Author manuscript

Cancer Res. Author manuscript; available in PMC 2021 June 15.

Published in final edited form as:

Cancer Res. 2020 December 15; 80(24): 5531–5542. doi:10.1158/0008-5472.CAN-20-0503.

Transient activation of the Hedgehog-Gli pathway rescues radiotherapy-induced dry mouth via recovering salivary gland resident macrophages

Qingguo Zhao[1,*], **Linying Zhang**[1,*], **Bo Hai**[1,*], **Jun Wang**[2], **Courtney L. Baetge**[3], **Michael A. Deveau**[3], **Geoffrey M. Kapler**[1], **Jian Q. Feng**[2], **Fei Liu**[1]

[1]Molecular and Cellular Medicine Department, College of Medicine, Texas A&M University Health Science Center, College Station, TX 77843, USA.

[2]Department of Biomedical Sciences, Texas A&M University College of Dentistry, Dallas, TX, 75246, USA.

[3]Department of Small Animal Clinical Sciences, College of Veterinary Medicine & Biomedical Sciences, Texas A&M University, College Station, TX 77843, USA.

Abstract

Irreversible hypofunction of salivary glands is a common side effect of radiotherapy for head-and-neck cancer and is difficult to remedy. Recent studies indicate that transient activation of Hedgehog signaling rescues irradiation-impaired salivary function in animal models, but the underlying mechanisms are largely unclear. Here we show in mice that activation of canonical Gli-dependent Hedgehog signaling by Gli1 gene transfer is sufficient to recover salivary function impaired by irradiation. Salivary gland cells responsive to Hedgehog/Gli signaling comprised small subsets of macrophages, epithelial cells and endothelial cells, and their progeny remained relatively rare long after irradiation and transient Hedgehog activation. Quantities and activities of salivary gland resident macrophages were substantially and rapidly impaired by irradiation and restored by Hedgehog activation. Conversely, depletion of salivary gland macrophages by clodronate liposomes compromised the restoration of irradiation-impaired salivary function by transient Hedgehog activation. Single cell RNA sequencing and qRT-PCR of sorted cells indicated that Hedgehog activation greatly enhances paracrine interactions between salivary gland resident macrophages, epithelial progenitors, and endothelial cells through Csf1, Hgf, and C1q signaling pathways. Consistently, expression of these paracrine factors and their receptors in salivary glands decreased following irradiation but were restored by transient Hedgehog activation. These findings reveal that resident macrophages and their pro-repair paracrine factors are essential for the rescue of irradiation-impaired salivary function by transient Hedgehog activation and are promising therapeutic targets of radiotherapy-induced irreversible dry mouth.

Graphical Abstract

Correspondence should be addressed to Fei Liu (fliu@tamu.edu). Address: 206 Olsen Blvd, 242B Reynolds Medical Bldg., College Station, TX 77843-1114. Telephone number: 979-436-9642 (office), 254-577-9382 (cell).

*These authors contribute equally to this manuscript.

Conflict of interest statement

The authors declare no potential conflicts of interest.

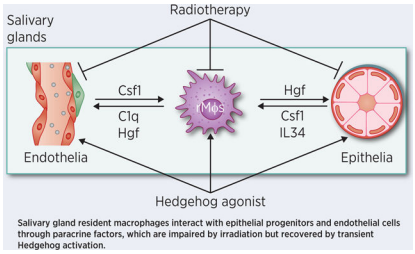

Salivary gland resident macrophages interact with epithelial progenitors and endothelial cells through paracrine factors, which are impaired by irradiation but recovered by transient Hedgehog activation.

Keywords

Hedgehog signaling; tissue-resident macrophages; radiotherapy; salivary glands; functional regeneration

Introduction

Radiotherapy for head and neck cancers (HNC) frequently exposes non-diseased salivary glands (SGs) to irradiation (IR), and consequently leads to irreversible salivary hypofunction (xerostomia) (1,2). IR-induced xerostomia exacerbates dental caries and periodontal disease and causes problems of taste, sleep and speech, which severely impair the quality of life. Available treatments for IR-induced xerostomia, such as artificial saliva and saliva secretion stimulators, can only temporarily relieve these symptoms.

Saliva secretion occurs in acinar epithelial cells and is dependent upon a rich blood supply by microvessels surrounding acini. IR causes the irreversible impairment of acinar epithelial cells and microvascular endothelial cells in SGs through multiple mechanisms (3–5). Among the three pairs of major salivary glands, submandibular glands (SMGs) produce two-thirds of the total volume of the whole saliva in the unstimulated state and ~46% of that after stimulation (6), and are the focus of many research studies including ours.

We found recently that IR-impaired salivary function can be rescued by the transient activation of Hedgehog signaling within SMGs. Hedgehog signaling is triggered by the binding of Hedgehog ligand proteins such as Sonic hedgehog (Shh) and Patched receptors (Ptch1/2). In the canonical Hedgehog signaling cascade, Hedgehog-Ptch binding derepresses the membrane protein Smoothened, which in turn promotes an increase in the active form of Gli transcription factors (full length Gli1/2/3) and decrease in the repressive form of Gli (truncated Gli2/3). Consequently, the increased ratio of active to repressive form of Gli factors induces the expression of Hedgehog target genes such as *Gli1* and *Ptch1* (7) (Supplementary Figure S1). Our previous studies revealed that the activity of canonical Hedgehog signaling in adult mouse SMGs is very low in the healthy state, increases following the obstructive damage that induces functional SG regeneration, but is unaffected by IR (8). We transiently activated the Hedgehog pathway after IR by inducible expression or adenovirus-mediated intra-SMG transfer of *Shh* gene, and observed that the long-term salivary function was rescued in both mouse and miniature pig models (9–12). Transient Hedgehog activation ameliorated IR-damage of SG epithelial and endothelial cells, but the direct cellular and molecular targets of Hedgehog activation in SGs remained unclear.

Here we report that the rescue of IR-impaired SG function by Hedgehog activation is through the recovery of SG-resident macrophages. In healthy adult mouse SGs, resident macrophages are abundant, derived from an embryonic origin but not from monocytes in circulation, and are homogeneously distributed throughout the SG (13,14). Similar macrophage-like cells are also abundant in healthy human SGs (15). We found that mouse SMG macrophages are responsive to canonical Hedgehog signaling, and their quantities and production of pro-regenerative paracrine factors are decreased by IR but restored or increased by transient activation of Hedgehog-Gli pathway following IR. Consistently, the depletion of SMG macrophages compromised rescue effects of Hedgehog activation on IR-impaired salivary function. These data not only reveal the mechanism of Hedgehog-mediated rescue, but also illuminate a novel direction for developing effective treatment of IR-induced xerostomia.

Materials and Methods

Animals

C57BL/6J, *Gli1-CreER*^{T2} and *Ai9(RCL-tdT)* mice were purchased from the Jackson Laboratory. All mouse procedures were approved by Texas A&M University IACUC. Sample number per group is based on our previous papers on rescue effects of intra-SMG transfer of Shh gene (10,11). Since Shh gene transfer rescued salivary function after irradiation with comparable efficiency in male and female mice (10), and >70% HNC patients are men (16), we used male mice in this study. 8–10 weeks old mice weighted between 25–30 grams were randomly grouped for treatments. The pilocarpine-stimulated whole saliva flow rates were measured as reported (9) by researchers blinded to treatments.

SG Irradiation

The IR parameters were determined through Helical Tomotherapy Planning and IR dose was verified with a solid-water phantom as detailed in the Supplementary Figures S2–S5. For IR, mice were anesthetized with ketamine/xylazine mixture at 0.1 mg ketamine and 0.01 mg xylazine per gram of body weight. The SGs of anesthetized mice was exposed to 15 Gy of 6 MeV electron beam produced by a medical linear accelerator (Clinac 2100C, Varian Medical Systems) as reported (11).

Preparation and delivery of adenoviral vectors into SMGs

Adenoviral vectors encoding green fluorescent protein (GFP), rat Shh or Gli1 (Applied Biological Materials) were expanded, purified and titered as reported (10). These vectors were delivered into SMGs of anesthetized mice by retroductal instillation as reported at a dose of 1×10^9 particles per gland on day 3 after IR (10).

Quantitative reverse transcription polymerase chain reaction (qRT-PCR)

RNAs were extracted from SMGs with RNeasy Mini Kit (Qiagen) and reversely transcribed with High-Capacity cDNA Reverse Transcription Kit (Applied Biosystems). The qPCR was performed with SYBR Green Master Mix (Bio-Rad) on a 7900HT Fast Real-Time PCR System (Applied Biosystems). The primers were synthesized by Invitrogen with sequences

retrieved from Primerbank (http://pga.mgh.harvard.edu/primerbank). The qPCR data were analyzed with *Rps9* as the reference gene using qBasePlus software (Biogazelle).

Western blot and ELISA

SMGs were homogenized with T-PRE reagent Tissue Protein Extraction Reagent (ThermoFisher, 40 μL per mg tissue) followed by centrifugation at 10,000 g for 5 min to collect supernatant. For western blot, proteins were fractionated by 12% sodium dodecyl sulfate-polyacrylamide gel electrophoresis, transferred to nitrocellulose membrane, and incubated with primary antibodies to Aqp5 (Abcam ab78486, 1:500) or Gapdh (Sigma-Aldrich, AB2302, 1:1,000). Bound primary antibodies were detected with horseradishperoxidase-conjugated secondary antibodies, observed by enhanced chemiluminescence (Pierce), photographed with VersaDoc imaging system, and quantified with QuantityOne software (Bio-Rad). The protein levels of Aif1, Cx3cr1, C1q and Csf1 were examined with corresponding ELISA kits (MyBioSource MBS922753 and MBS3805156, Lifespan F8963, and Invitrogen EMCSF1) following manufacturers' instructions.

RNA sequencing (RNA-seq) and bioinformatics analyses

RNA-seq library preparation and sequencing were outsourced to NeoGenomics Labs (Houston, TX). Briefly, the tissue samples underwent RNA isolation using Qiagen RNeasy Mini Kit, and RNA quality was confirmed with Agilent Bioanalyzer RNA Nano Kit with RIN >7. The Illumina TruSeq Stranded mRNA Sample Prep Kit instructions were followed to generate barcoded RNA sequencing libraries. These libraries were pooled in equal molar ratio and processed using a standard Illumina HiSeq 2500 pipeline. The bioinformatics analyses were performed by researchers blinded to treatments with methods described in the Supplementary Methods.

Flow cytometry

Cells were isolated from mouse SMG as reported (14). Briefly, SMGs were isolated, minced, and digested for 1 h with RPMI 1640 medium containing 1mg/ml of collagenase IV, 5mM $CaCl_2$, 50mg of DNase I and 8% fetal bovine serum with continuous shaking at room temperature. For examining macrophage subpopulations, cells were stained with FITC-labeled Ly6C antibody, PE-labeled F4/80 antibody or corresponding isotype controls (BD Pharmingen, 553104, 565410, 553942 and 553930, 1:100). For sorting, cells were stained with FITC-labeled antibodies for CD31 or Epcam (Biolegend 102405 and 118207, 1:100), PE-labeled F4/80 antibody mentioned above or corresponding isotype controls. Dead cells were excluded with LIVE/DEAD Fixable Aqua Dead Cell Stain Kit (Invitrogen).

Single cell RNA sequencing (scRNA-seq) and bioinformatics analyses

Single cell suspensions from mouse SMGs were generated as mentioned above. scRNA-seq libraries were generated in TAMU Genomics Core using the 10x Chromium platform and the version 3 Chromium Single Cell 3' reagent kit following the manufacturer's instructions (10x Genomics). Samples were pooled in equimolar concentrations and sequenced on a single lane of an S4 2×150 PE flow cell for an Illumina NovaSeq 6000. 11,048 and 18,333

cells from GFP and Shh groups were sequenced to a depth of 43,924 mean reads per cell and 1,420 median genes per cell. The bioinformatics analyses were performed by researchers blinded to treatments with methods described in the Supplementary Methods. The Uniform Approximation and Projection method (UMAP) was used to visualize the clusters. Putative T cells and B cells are abnormally abundant in GFP sample only likely due to blood contamination and are excluded from further analyses. Normalized data are shown in the form of feature plots.

Lineage tracing and immunofluorescence (IF) staining

8–10 weeks old *Gli1-CreER^{T2};Ai9(RCL-tdT)* mice were subjected to 15 Gy IR at the SG region or mock treatment. At 3 days after IR, these mice were transduced with AD-GFP or Ad-Shh as mentioned above, and then injected with 100 μg 4-hydroxytamoxifen (4-OHT, Sigma) daily for 3 days. Mice were euthanized to collect SMGs 7 or 42 days after 4-OHT induction. Frozen SMG sections were first incubated in PBS or a 1:100 dilution of following primary antibodies: Aif1/Iba1 (Abcam ab48004), Krt5 (BioLegend 905901), Cd31 (BD Pharmingen 558736), Krt8 (Novus Biologicals NBP216094) or Aqp5 (Abcam ab78486) at 4°C overnight. Sections were then washed and incubated with appropriate secondary antibodies labeled with Cy7 (Vector Laboratories), and counterstained with DAPI. Sections were imaged using a fluorescent microscopy (Nikon, Eclipse 80i), and were analyzed with NIS Elements software.

Depletion of SMG macrophages

Based on published protocols (17–19), clodronate liposomes (CL, 50 μg/mL, FormuMax) and control liposomes were IV injected (0.2 ml) into mice on Day 2 and 4 after IR or mock treatment, and directly injected into SMGs (0.03 ml per gland at 3 sites) on Day 4. SMGs were collected 3 days after last CL injection from some mice for flow cytometry assay. Other mice were transduced with Ad-Shh as mentioned above.

Statistics

No animals or samples were excluded from the final analysis and samples were not pooled for analyses. The numbers of experimental replicates are 3 for RNA-seq and 5 for all other assays, and technical replicates are 3 for qRT-PCR and ELISA and 2 for flow cytometry and western blot. All statistical analysis and graphical generation of data were performed with GraphPad Prism software. All quantified data were analyzed with nonparametric Kruskal-Wallis test followed by the Dunn’s post test.

Results

Transient activation of Gli-dependent canonical Hedgehog signaling is sufficient to rescue IR-impaired salivary function.

Besides the canonical signaling cascade mediated by Gli transcription factors, Hedgehog ligands are capable of triggering several Gli-independent non-canonical signaling cascades (20). To determine whether transient activation of Gli-dependent canonical Hedgehog signaling is able to rescue IR-impaired salivary function, we performed 15 Gy local IR to the neck region containing all major SGs in 8–10 weeks old C57BL/6 mice. On day 3 after IR,

we delivered adenoviral vectors (Ad) carrying cDNA of rat Gli1, rat Shh or GFP into SMGs by retroductal instillation as reported (10). In mice, it is technically challenging to measure resting saliva flow rate or gland-specific stimulated saliva flow rate, therefore we measured the stimulated whole saliva flow rates as a key SMG function readout at 28, 60 or 90 days after IR, and collected SMG samples at 7, 14, 28 or 90 days after IR (Fig. 1A). In SMGs collected 7 days after IR, the expression of Hedgehog target genes, mouse *Gli1* and *Ptch1* (7), was not significantly affected by IR or IR plus Ad-GFP treatment, but significantly increased in IR plus Ad-Gli1 or Ad-Shh groups compared with IR or non-treated (NT) groups (Fig. 1B–C), which confirmed the effective activation of Hedgehog-Gli pathway by Ad-Gli1. The higher levels of Hedgehog target genes in Gli1 group compared with Shh group at day 7 were likely due to the additional Hedgehog activation in SMG cells not expressing functional Hedgehog receptors. In SMGs collected 14 or 28 days after IR, the expression of these two Hedgehog target genes was not significantly affected by any treatment, indicating that Ad-Gli1 delivery activated Hedgehog signaling in irradiated SMGs transiently as Ad-Shh did (10). Local IR progressively decreased the stimulated whole saliva flow rates from day 28 to day 90 as expected, and significantly reduced the expression of acinar marker Aquaporin 5 (Aqp5) in SMGs by 90 days after IR at both mRNA and protein levels (Fig. 1D–G). Both salivary function indexes were significantly rescued by the intra-SMG delivery of Ad-Shh or Ad-Gli1 with comparable efficacies (Fig. 1D–G). Since all three pairs of major SGs were exposed to IR and only SMGs were treated, considering the ~46% contribution of stimulated saliva from SMGs (6), the ~40% stimulated whole saliva flow rates indicate an effective rescue of SMG function in Shh and Gli1 groups by day 90 (Fig. 1D). These data confirm that transient activation of canonical Hedgehog signaling is sufficient to rescue IR-impaired salivary function.

Gli1$^+$ Hedgehog-responsive cells in SMGs comprise small subsets of macrophages, epithelial cells and endothelial cells during homeostasis and repair after IR damage.

To identify cells that directly respond to canonical Hedgehog signaling in SMGs, we used *Gli1-CreER^{T2};Ai9(RCL-tdT)* mice that carry Cre-inducible tdTomato (tdT) gene in the Rosa26 locus. After Cre activation with 4-hydroxytamoxifen (4-OHT), Gli1-expressing Hedgehog-responsive cells and their progeny will be labeled with tdT$^+$ in these mice (21). At 3 days before 4-OHT treatment, some mice was firstly treated with 15 Gy IR at the head and neck region. On the same day before 4-OHT treatment, some irradiated mice received intra-SMG transfer of Ad-GFP or Ad-Shh as mentioned above. 4-OHT was adminstrated intraperitoneally (IP) and daily from day 0 to 2, and SMGs were collected in 7 and 42 days for section (Fig. 2A). In both day 7 and 42 SMGs, compared with non-treated (NT) samples, tdT$^+$ cells were slightly decreased by IR or IR+GFP, but significantly increased by IR+Ad-Shh (Fig. 2B–E). In all day 7 SMGs, tdT$^+$ cells were rare and sparsely distributed in the stroma, basal epithelia and vessel-like structures (Fig. 2B). Compared with day 7 samples, in day 42 SMGs with the same treatment, tdT$^+$ cells greatly increase, become more concerntrated, and form ring-shaped structures or cord-like structures adjecent to large ducts, but are still relatively rare (Fig. 2B–E). At all samples at both time points, immunoflourescent staining (IF) indicated tdT$^+$ cells express macrophage marker Aif1/Iba1, basal/myo-epithelial marker Keratin-5 (Krt5), or endothelial marker Cd31/Pecam1 (Fig. 2F–K). These tdT$^+$ cells are rarely positive for duct marker Krt8 and negative for acinar marker

Aqp5 at both day 7 and 42, but form ring-shaped structures surronding some $Krt8^+$ ducts or $Aqp5^+$ acini at day 42 (Supplementary Fig. S6A–D). These data indicate that cord-like and ring-shaped structures are microvessels and interconnected macrophages (14) or myoepithelial cells. Collectively, our lineage tracing data suggest that $Gli1^+$ Hedgehog-responsive cells in SMGs comprise small subset of macrophages, basal/myo-epithelial cells and endothelial cells, and these cells expand to a limited extent during recovery from IR damage even after transient Hedgehog activation.

SMG-resident macrophages were decreased by IR but restored by Hedgehog activation following IR.

To find clues for underlying mechanisms of Hedgehog-mediated rescue of IR-impaired salivary function, we collected SMGs from all 5 treatment groups mentioned in Figure 1 at 7 days after IR for high throughput RNA sequencing (RNA-seq). The RNA-seq dataset has been deposited to GEO with the record number GSE133482. The differentially expressed genes in each group vs. NT or IR only group respectively were identified (Supplementary file 2) and subjected to Ingenuity Pathway Analysis (IPA). The p53 signaling activity is elevated by DNA damages following IR for weeks (22) and not affected by intra-SMG Shh gene transfer (11). As indicated by the analysis of canonical pathways, p53 signaling is activated in all groups treated with IR to comparable extents (Fig. 3A), which is confirmed by qRT-PCR assays on p53 target genes Cdkn1a/p21, Mdm2 and Trp53inp1 (Fig. S7A–C), indicating that IR injury levels are comparable between different treatment groups. Notably, IR inhibited multiple macrophage-related pathways, including pattern recognition, phagocytosis, GM-CSF (Csf2) signaling essential for the maintenance of tissue-resident macrophages (23), and HGF signaling related to pro-repair effects of macrophages (24) (Fig. 3A). These IR-inhibited pathways were restored or activated by intra-SMG gene transfer of Shh or Gli1 but not by GFP (Fig. 3A). As indicated by the analysis of biological functions, IR inhibited angiogenesis as reported (3), and reduced quantity and proliferation of mononuclear leukocytes, phagocytosis of myeloid cells, and activation of phagocytes, whereas Shh or Gli1 but not GFP gene transfer after IR restored or enhanced these functions compared with IR treatment alone (Fig. 3B).

To validate these RNA-seq data, we performed flow cytometry analysis of macrophage markers in SMGs of adult C57BL/6 mice collected 3 or 7 days after IR with or without intra-SMG transfer of GFP or Shh gene. $F4/80^+$ macrophages are abundant in NT SMGs and most of them (>85%) are resident macrophages (rMϕ) as indicated by the low expression of Ly6c (25) (Fig. 3C–D). IR significantly decreased numbers of $F4/80^+/Ly6c^{low}$ resident macrophages but not $F4/80^+/Ly6c^{high}$ infiltrating macrophages (iMϕ) by 3 and 7 days, whereas Shh but not GFP gene delivery restored this index (Fig. 3C–E). The percentages of $F4/80^+/Ly6c^{high}$ infiltrating macrophages increased in Shh and GFP groups compared with NT or IR SMGs, but were still much lower than those of $F4/80^+/Ly6c^{low}$ resident macrophages (Fig. 3C–E), suggesting that their increases are likely caused by the delivery of adenoviral vectors and less essential for salivary function than resident macrophages. Quantitative RT-PCR data confirmed that IR significantly down-regulated the mRNA levels of macrophage markers (Cd11c, F4/80, Aif1/Iba1 and Fcgr1), phagocytosis receptors (Fcgr1 and Axl) and tissue-resident macrophage marker Cx3cr1 (26) by 3 and 7 days, whereas

transfer of Shh or Gli1 but not GFP gene after IR restored or increased them on day 7 (Fig. 3F). Consistent changes of Aif1 and Cx3cr1 proteins were validated with ELISA (Fig. 3G–H). These data demonstrate that IR severely impaired SG-resident macrophages, whereas Hedgehog activation following IR restored them.

The depletion of SG macrophages abolished Hedgehog-mediated rescue of salivary function following IR.

To determine whether SG macrophages are required for Hedgehog-mediated rescue of salivary function after IR, we depleted SMG macrophages with clodronate liposomes (CL) as reported (17–19) one day after intra-SMG transfer of Shh or 4 days after IR (Fig. 4A). In SMGs collected 3 days after CL injection with or without IR or IR+Shh, flow cytometry indicated that CL efficiently depleted both $Ly6c^{low}$ and $Ly6c^{high}$ $F4/80^{+}$ macrophages (resident and infiltrating macrophages, >45% decrease) in all three groups (Fig. 4B–D). The stimulated saliva flow rate were measured at 90 days after IR or corresponding mock treatment (NT), and SMGs were collected at day 90 to examine the level of acinar marker Aqp5. At 90 days after treatment, mice subjected to CL injection alone maintained their saliva production and the mRNA and protein expression of Aqp5 in SMGs at levels comparable to NT group, while mice subjected to IR plus CL injection showed decreases of both indexes comparable to IR group (Fig. 4E–H). Notably, in mice subjected to Shh gene transfer plus CL injection after IR, these two indexes are comparable to IR group and significantly lower than the IR+Shh group (Fig. 4E–H). These data indicate that SMG macrophages are required for the rescue of salivary function by transient Hedgehog activation following IR.

Hedgehog activation promoted paracrine interactions of macrophages with epithelial progenitors and endothelial cells.

To determine how Hedgehog-Gli signaling regulates SG function through macrophages, we performed single cell RNA sequencing (scRNA-seq) of adult mouse SMGs harvested 7 days after intra-SMG delivery of Ad-Shh or Ad-GFP. The identities of cell clusters were determined by the expression of marker genes as reported (27,28) (Fig. 5A and Supplementary Table 1). The cells responsive to Hedgehog-Gli signaling were identified by expression of *Ptch1*, the Hedgehog receptor and target gene. In the GFP group, $Ptch1^{+}$ cells are mostly enriched in putative resident macrophages (rMp, $Cx3cr1^{+}Ccr2^{-}$, Fig. S8A) (26), and are moderately enriched in innate lymphoid cells (ILCs) (29), ductal cells and endothelia cells (Fig. 5A–B). In the Shh group, $Ptch1^{+}$ cells strikingly increased in endothelial cells, acinar/ductal progenitors (ADP, $Aqp5^{+}/Krt8^{+}/Epcam^{high}$), and ductal progenitors (DP, $Krt8^{+}/Epcam^{high}$ and $Ascl3^{+}$ or $Sox9^{+}$) (28), and moderately increased in ILCs, basal/myo-epithelial cells, and mesenchymal stem cells (MSCs) (Fig. 5A–B). Meanwhile, Hedgehog activation strikingly increased percentages of ADP, DP and endothelial cells in all SMG cells, and moderately increased those of basal/myo-epithelial cells, MSCs and rMp, but did not increase that of ILCs (Fig. 5C). However, Hedgehog activation did not significantly increase the levels of proliferation markers *Pcna* and *Mki67* in all $Ptch1^{+}$ cells or $Ptch1^{+}$ endothelial cells ($P > 0.05$), and only a small percentage of $Mki67^{+}$ cells *are* $Ptch1^{+}$ (Fig. S8B). These data suggest that Hedgehog activation likely expanded these cells through indirect mechanisms.

Macrophages or monocytes were reported to promote proliferation of cultured intestine epithelial cells and endothelial cells through HGF-Met signaling (24,30). In mouse SMGs HGF-Met signaling is inhibited by IR but upregulated by Hedgehog activation after IR (Fig. 3A). Consistently, scRNA-seq indicated that *Hgf*$^{+}$ cells are enriched in putative resident macrophages with or without Hedgehog activation, and increased greatly by Hedgehog activation (Fig. 5D–E). Without Hedgehog activation, *Met/Hgfr*$^{+}$ cells are rarely present in putative endothelial cells, ductal cells, ADP and DP; after Hedgehog activation, *Met/Hgfr*$^{+}$ cells greatly increased in ADP, DP and endothelial cells (Fig. 5D–E). Another potential pro-repair factor produced by macrophages is C1q that promote angiogenesis through C1q receptor Cd93/C1qRP on endothelial cells (31,32). With or without Hedgehog activation, cells express all *C1q* genes (*C1qa, C1qb* and *C1qc*) at high levels (>50th percentile) are mainly putative SMG-resident macrophages, whereas *Cd93* expression is enriched in putative endothelial cells without Hedgehog activation and increased strikingly in these cells by Hedgehog activation (Fig. 5D–E). The maintainance of tissue-resident macrophages is regulated by Csf1/IL34-Csf1r and Csf2-Csf2r signaling (23). In SMGs with or without Hedgehog activation, *Csf1r*^{high} (>50th percentile) cells are mainly putatvie resident macrophages (Fig. 5D), and majority of resident macrophages (>70%) expressing only *Csf1r* but not *Csf2r* (Fig. S8C). In SMGs without Hedgehog activation, *Csf1*$^{+}$ cells are much more abundant than *IL34*$^{+}$ cells and *Csf2*$^{+}$ cells, and Hedgehog activation greatly increased the percentages of *Csf1*$^{+}$ and *IL34*$^{+}$ cells in all SMG cells, but did not significantly affect that of *Csf2*$^{+}$ cells (Fig. 5D–E and Fig. S8D). After Hedgehog activation, both *Csf1*$^{+}$ cells and *IL34*$^{+}$ cells are enriched in the putative ADP, DP and basal/myo-epithelial cells, whereas *Csf1*$^{+}$ cells are also enriched in the putative endothelial cells (Fig. 5D–E). The increases of above genes by Hedgehog activation are found in both *Ptch1*$^{+}$ and *Ptch1*$^{-}$ cells (Fig. 5F), suggesting that Hedgehog activation induces these genes both directly and indirectly.

To validate the cell type specific expression of these factors, we sorted F4/80^{+} macrophages, Cd31^{+} endothelial cells, and Epcam^{high} putative epithelial progenitor cells by flow cytometry from SMGs at 7 days after Ad-GFP or Ad-Shh treatment, and examined the expression of these factors with qRT-PCR assays. Compared with cells negative or low for the corresponding marker with or without Hedgehog activation, F4/80^{+} macrophages express significantly higher levels of *C1qa, C1qb, C1qc, Csf1r* and *Hgf* (Fig. S9A), Epcam^{high} cells express significantly higher levels of *IL34* and *Met/Hgfr* (Fig. S9B), and Cd31^{+} endothelial cells express significantly higher levels of *Csf1* and *Cd93/C1qRP* in both groups and higher level of *Met/Hgfr* in Shh group alone (Fig. S9C). Notably, Ad-Shh treatment significantly increased the relative levels of *C1q* factors, *Csf1r* and *Hgf* in macrophages compared with Ad-GFP treatment, suggesting the activation of macrophages after Hedgehog activation. These data together suggest that Hedgehog activation triggers positive feedback loops between epithelial progenitors, endothelia cells and resident macrophages through Csf1/IL34, Hgf and C1q signaling pathways.

IR impaired paracrine interactions of SG-resident macrophages with epithelial and endothelial cells, and Hedgehog activation following IR restored them.

To determine effects of IR and transient Hedgehog activation following IR on above paracrine interactions, we examined the mRNA expression of these genes and the tissue-

resident macrophage marker *Cx3cr1* by qRT-PCR in SMGs at day 3, 7, 14 and 28 after IR with or without intra-SMG Ad-Shh treatment on day 3. Consistent to data in Figure 3, the mRNA expression of macrophage-enriched Csf1r, Cx3cr1, C1qa and Hgf was significantly decreased by IR compared with the NT group, and was significantly increased by Shh but not GFP gene transfer compared with the IR group at day 7 and 14 (Fig. 6A–D). At day 28, the mRNA expression of Cx3cr1, C1qa and Hgf was still significantly down-regulated by IR and recoverd by Shh but not GFP gene transfer. The mRNA expression of Csf1r ligands (Csf1 and IL34), proangiogenic C1q receptor CD93 and Hgf receptor Met was significantly decreased by IR at day 14 or 28 compared with the NT group, and was significantly increased by Shh but not GFP gene transfer compared with the IR group at day 7, 14 and 28 except the slight increase of *Met* at day 7 (Fig. 6E–H). The consistent changes of C1q and Csf1 proteins were confirmed by ELISA at day 3 and 7 after IR (Fig. 6I–J). These data indicate that consequent to acute IR damages to SMG cells, IR leads to persistent defects of paracrine interactions between resident macrophages, epithelial progenitors and endothelial cells; conversely, transient Hedgehog activation after IR enhance these paracrine interactions rapidly and for a prolonged period (Fig. 6K). Since transient Hedgehog activation rescues salivary function after IR through preserving epithelial stem/progenitor cells and promoting angiogenesis (9–12), whereas SG macrophages are required for such a rescue (Fig. 4), these data suggest that the macrophage-derived proangiogenic and pro-repair factors, C1q and Hgf, likely play essential roles in the rescue of salivary function by Hedgehog activation.

Discussion

Current research on molecular therapies of the IR-induced salivary hypofunction mainly focus on recovering the impaired acinar epithelial cells or microvascular endothelial cells (33). Resident macrophages with an embryonic origin are essential for functional repair of multiple orgnas (34,35) and abundant in SGs (13–15), but their roles in IR damages and function restoration of SGs have never been explored. We report here that IR greatly impairs SG-resident macrophages and decreases expression of macrophage-derived pro-regenerative factors Hgf and C1q and their receptors. We also found that Hedgehog activation after IR recovers SG-resident macrophages, either directly or through inducing expression of Csf1 and IL34 in epithelial progenitors and endothelial cell, which in turn restore the expression of macrophage-derived Hgf and C1q. Conversely, the depletion of SG macrophages abolished rescue effects of tranisent Hedgehog activation on salivary function following IR. These data indicate that SG-resident macrophages are essential for the fuctional SG regeneration following IR, which is related to their paracrine interactions with epithelial progenitors and endothelial cells.

Besides these paracrine interactions, SG-resident macrophages likely also contribute to the restoration of salivary function after IR through pro-regenerative innate immune responses. These responses include the regulation of inflammation caused by IR and the removal of cell debris and dead or senescent cells, and are essential for functional regeneration of several other organs (36,37). Notably, C1q also enhances phagocytosis by tagging damage-associated molecular patterns and apoptotic cells (38), and promotes the polarization of macrophages to the M2 phenotype and the production of anti-inflammatory cytokines (39). Therefore the recovery of resident macrophages and C1q expression in irradiated SMGs by

transient Hedgehog activation might restore salivary function through both direct pro-repair effects and indirect innate immune responses. The contributions of the latter to the restoration of salivary function are worth further study.

We reported previously that transient activation of Hedgehog pathway following IR rescues salivary function through preservation of salivary epithelial stem/progenitor cells, endothelial cells and parasympathetic innervation mainly via non-cell-autonomous mechanisms such as inhibiting cellular senescence and inducing pro-repair paracrine factors (9–11), but SG cells directly responsive to Hedgehog activation are unclear. As indicated by findings reported here, Hedgehog-responsive cells are much more abundant in SG-resident macrophages than in all other types of SG cells including epithelial and endothelial cells (Fig. 5A–B), and the preservation of salivary epithelial stem/progenitor cells and endothelial cells appears largely mediated through the recovery of SG-resident macrophages and their pro-repair paracrine factors (Figures 4–6). Meanwhile, as reported in other tissues, the recovery of resident macrophages in SGs likely also contributes to the preservation of parasympathetic innervation and the inhibition of cellular senescence by transient Hedgehog activation. The underlying mechanisms include clearing axonal debris (36) and senescent cells (37), promoting neurite outgrowth (40), enhancing DNA repair through Hgf (41) and resolving inflammation that propagates DNA damage and senescence (42).

Present approaches of preserving SG acinar epithelial cells or endothelial cells after IR rely on anti-apoptosis factors, growth factors and angiogenic factors. These factors generally have pro-tumor risks when their levels increase in blood or tumor (33), which limits their application in HNC survivors. Our findings indicate that SG-resident macrophages and their paracrine factors are essential for the recovery of IR-impaired salivary function. These cells and factors could be manipulated safely in cancer patients. For instances, Csf2/GM-CSF that regulates the survival and proliferation of resident macrophages (23) has been approved by FDA for applications in cancer patients (43); while C1q, a major pro-repair factor secreted by SG-resident macrophages, also appears safe for application in cancer patients (44). Therefore, it will be worth exploring whether recovering SG-resident macrophages and/or their paracrine factors is sufficient to restore salivary function following radiotherapy.

In summary, our studies demonstrate that SG-resident macrophages are essential for the Hedgehog-mediated restoration of the IR-impaired salivary function, which is related to their paracrine interactions with endothelial and epithelial cells. These findings shed light on a new research direction for the development of safer and more effective treatments of radiotherapy-induced salivary hypofunction in HNC survivors.

Supplementary Material

Refer to Web version on PubMed Central for supplementary material.

ACKNOWLEDGMENTS

This study was supported by NIH/NIDCR 1R01DE022975-01 to Q. Zhao, B. Hai and F. Liu and TAMHSC bridge fund to F. Liu. We sincerely thank Drs. Andrew Hillhouse and Kranti Konganti in TAMU Genomics Core for scRNA-seq. F.L conceived the study; Q.Z and B.H. performed most experiments; L.Z. performed bioinformatics analyses; J.W. contributed to animals and protocols for lineage tracing; C.L.B and M.A.D. performed mouse

irradiation; J.Q.F., G.M.K. and F.L. supervised experiments in their laboratories, analyzed the corresponding data and wrote the manuscript.

References:

1. Jensen SB, Pedersen AM, Vissink A, Andersen E, Brown CG, Davies AN, et al. A systematic review of salivary gland hypofunction and xerostomia induced by cancer therapies: management strategies and economic impact. Supportive care in cancer : official journal of the Multinational Association of Supportive Care in Cancer 2010;18:1061–79 [PubMed: 20333412]
2. Ghosh-Laskar S, Yathiraj PH, Dutta D, Rangarajan V, Purandare N, Gupta T, et al. Prospective randomized controlled trial to compare 3-dimensional conformal radiotherapy to intensity-modulated radiotherapy in head and neck squamous cell carcinoma: Long-term results. Head Neck 2015
3. Cotrim AP, Sowers A, Mitchell JB, Baum BJ. Prevention of irradiation-induced salivary hypofunction by microvessel protection in mouse salivary glands. Mol Ther 2007;15:2101–6 [PubMed: 17726456]
4. Marmary Y, Adar R, Gaska S, Wygoda A, Maly A, Cohen J, et al. Radiation-Induced Loss of Salivary Gland Function Is Driven by Cellular Senescence and Prevented by IL6 Modulation. Cancer Res 2016;76:1170–80 [PubMed: 26759233]
5. Avila JL, Grundmann O, Burd R, Limesand KH. Radiation-induced salivary gland dysfunction results from p53-dependent apoptosis. Int J Radiat Oncol Biol Phys 2009;73:523–9 [PubMed: 19147016]
6. Proctor GB. The physiology of salivary secretion. Periodontology 2000 2016;70:11–25 [PubMed: 26662479]
7. Pandolfi S, Stecca B. Cooperative integration between HEDGEHOG-GLI signalling and other oncogenic pathways: implications for cancer therapy. Expert Rev Mol Med 2015;17:e5 [PubMed: 25660620]
8. Hai B, Yang Z, Millar SE, Choi YS, Taketo MM, Nagy A, et al. Wnt/beta-catenin signaling regulates postnatal development and regeneration of the salivary gland. Stem Cells Dev 2010;19:1793–801 [PubMed: 20367250]
9. Hai B, Qin L, Yang Z, Zhao Q, Shangguan L, Ti X, et al. Transient activation of hedgehog pathway rescued irradiation-induced hyposalivation by preserving salivary stem/progenitor cells and parasympathetic innervation. Clin Cancer Res 2014;20:140–50 [PubMed: 24150232]
10. Hai B, Zhao Q, Qin L, Rangaraj D, Gutti VR, Liu F. Rescue Effects and Underlying Mechanisms of Intragland Shh Gene Delivery on Irradiation-Induced Hyposalivation. Hum Gene Ther 2016;27:390–9 [PubMed: 27021743]
11. Hai B, Zhao Q, Deveau MA, Liu F. Delivery of Sonic Hedgehog Gene Repressed Irradiation-induced Cellular Senescence in Salivary Glands by Promoting DNA Repair and Reducing Oxidative Stress. Theranostics 2018;8:1159–67 [PubMed: 29464006]
12. Hu L, Zhu Z, Hai B, Chang S, Ma L, Xu Y, et al. Intragland Shh gene delivery mitigated irradiation-induced hyposalivation in a miniature pig model. Theranostics 2018;8:4321–31 [PubMed: 30214623]
13. Pappo J, Ebersole JL, Taubman MA. Resident salivary gland macrophages function as accessory cells in antigen-dependent T-cell proliferation. Immunology 1988;63:99–104 [PubMed: 2828229]
14. Thom JT, Walton SM, Torti N, Oxenius A. Salivary gland resident APCs are Flt3L- and CCR2-independent macrophage-like cells incapable of cross-presentation. Eur J Immunol 2014;44:706–14 [PubMed: 24271944]
15. Le A, Saverin M, Hand AR. Distribution of dendritic cells in normal human salivary glands. Acta histochemica et cytochemica 2011;44:165–73 [PubMed: 21927515]
16. Siegel RL, Miller KD, Jemal A. Cancer statistics, 2020. CA Cancer J Clin 2020;70:7–30 [PubMed: 31912902]
17. Wang S, Baum BJ, Kagami H, Zheng C, O'Connell BC, Atkinson JC. Effect of clodronate on macrophage depletion and adenoviral-mediated transgene expression in salivary glands. J Oral Pathol Med 1999;28:145–51 [PubMed: 10235366]

18. Weisser SB, van Rooijen N, Sly LM. Depletion and reconstitution of macrophages in mice. J Vis Exp 2012:4105 [PubMed: 22871793]
19. Kozicky LK, Sly LM. Depletion and Reconstitution of Macrophages in Mice. Methods Mol Biol 2019;1960:101–12 [PubMed: 30798525]
20. Brennan D, Chen X, Cheng L, Mahoney M, Riobo NA. Noncanonical Hedgehog signaling. Vitamins and hormones 2012;88:55–72 [PubMed: 22391299]
21. Jing Y, Li C, Feng JQ. Application of Cell Lineage Tracing Combined with Immunofluorescence in the Study of Dentinogenesis. Methods Mol Biol 2019;1922:39–48 [PubMed: 30838563]
22. Di Leonardo A, Linke SP, Clarkin K, Wahl GM. DNA damage triggers a prolonged p53-dependent G1 arrest and long-term induction of Cip1 in normal human fibroblasts. Genes Dev 1994;8:2540–51 [PubMed: 7958916]
23. Hashimoto D, Chow A, Noizat C, Teo P, Beasley MB, Leboeuf M, et al. Tissue-resident macrophages self-maintain locally throughout adult life with minimal contribution from circulating monocytes. Immunity 2013;38:792–804 [PubMed: 23601688]
24. D'Angelo F, Bernasconi E, Schafer M, Moyat M, Michetti P, Maillard MH, et al. Macrophages promote epithelial repair through hepatocyte growth factor secretion. Clinical and experimental immunology 2013;174:60–72 [PubMed: 23773083]
25. Arnold L, Henry A, Poron F, Baba-Amer Y, van Rooijen N, Plonquet A, et al. Inflammatory monocytes recruited after skeletal muscle injury switch into antiinflammatory macrophages to support myogenesis. J Exp Med 2007;204:1057–69 [PubMed: 17485518]
26. Epelman S, Lavine KJ, Beaudin AE, Sojka DK, Carrero JA, Calderon B, et al. Embryonic and adult-derived resident cardiac macrophages are maintained through distinct mechanisms at steady state and during inflammation. Immunity 2014;40:91–104 [PubMed: 24439267]
27. Song EC, Min S, Oyelakin A, Smalley K, Bard JE, Liao L, et al. Genetic and scRNA-seq Analysis Reveals Distinct Cell Populations that Contribute to Salivary Gland Development and Maintenance. Scientific reports 2018;8:14043 [PubMed: 30232460]
28. Oyelakin A, Song EAC, Min S, Bard JE, Kann JV, Horeth E, et al. Transcriptomic and Single-Cell Analysis of the Murine Parotid Gland. J Dent Res 2019;98:1539–47 [PubMed: 31623513]
29. Cortez VS, Cervantes-Barragan L, Robinette ML, Bando JK, Wang Y, Geiger TL, et al. Transforming Growth Factor-beta Signaling Guides the Differentiation of Innate Lymphoid Cells in Salivary Glands. Immunity 2016;44:1127–39 [PubMed: 27156386]
30. Schubert SY, Benarroch A, Ostvang J, Edelman ER. Regulation of endothelial cell proliferation by primary monocytes. Arteriosclerosis, thrombosis, and vascular biology 2008;28:97–104
31. Bossi F, Tripodo C, Rizzi L, Bulla R, Agostinis C, Guarnotta C, et al. C1q as a unique player in angiogenesis with therapeutic implication in wound healing. Proc Natl Acad Sci U S A 2014;111:4209–14 [PubMed: 24591625]
32. Du J, Yang Q, Luo L, Yang D. C1qr and C1qrl redundantly regulate angiogenesis in zebrafish through controlling endothelial Cdh5. Biochem Biophys Res Commun 2017;483:482–7 [PubMed: 28007601]
33. Nair RP, Sunavala-Dossabhoy G. Promising Gene Therapeutics for Salivary Gland Radiotoxicity. AIMS medical science 2016;3:329–44 [PubMed: 28286865]
34. De Schepper S, Verheijden S, Aguilera-Lizarraga J, Viola MF, Boesmans W, Stakenborg N, et al. Self-Maintaining Gut Macrophages Are Essential for Intestinal Homeostasis. Cell 2018;175:400–15 e13 [PubMed: 30173915]
35. Puranik AS, Leaf IA, Jensen MA, Hedayat AF, Saad A, Kim KW, et al. Kidney-resident macrophages promote a proangiogenic environment in the normal and chronically ischemic mouse kidney. Scientific reports 2018;8:13948 [PubMed: 30224726]
36. Peluffo H, Solari-Saquieres P, Negro-Demontel ML, Francos-Quijorna I, Navarro X, Lopez-Vales R, et al. CD300f immunoreceptor contributes to peripheral nerve regeneration by the modulation of macrophage inflammatory phenotype. Journal of neuroinflammation 2015;12:145 [PubMed: 26259611]
37. Egashira M, Hirota Y, Shimizu-Hirota R, Saito-Fujita T, Haraguchi H, Matsumoto L, et al. F4/80+ Macrophages Contribute to Clearance of Senescent Cells in the Mouse Postpartum Uterus. Endocrinology 2017;158:2344–53 [PubMed: 28525591]

38. Verneret M, Tacnet-Delorme P, Osman R, Awad R, Grichine A, Kleman JP, et al. Relative contribution of c1q and apoptotic cell-surface calreticulin to macrophage phagocytosis. Journal of innate immunity 2014;6:426–34 [PubMed: 24557008]

39. Benoit ME, Clarke EV, Morgado P, Fraser DA, Tenner AJ. Complement protein C1q directs macrophage polarization and limits inflammasome activity during the uptake of apoptotic cells. Journal of immunology 2012;188:5682–93

40. Zigmond RE, Echevarria FD. Macrophage biology in the peripheral nervous system after injury. Progress in neurobiology 2019;173:102–21 [PubMed: 30579784]

41. Fan S, Ma YX, Wang JA, Yuan RQ, Meng Q, Cao Y, et al. The cytokine hepatocyte growth factor/scatter factor inhibits apoptosis and enhances DNA repair by a common mechanism involving signaling through phosphatidyl inositol 3' kinase. Oncogene 2000;19:2212–23 [PubMed: 10822371]

42. Lasry A, Ben-Neriah Y. Senescence-associated inflammatory responses: aging and cancer perspectives. Trends in immunology 2015;36:217–28 [PubMed: 25801910]

43. Yu WL, Hua ZC. Evaluation of effectiveness of granulocyte-macrophage colony-stimulating factor therapy to cancer patients after chemotherapy: a meta-analysis. Oncotarget 2018;9:28226–39 [PubMed: 29963274]

44. Mangogna A, Agostinis C, Bonazza D, Belmonte B, Zacchi P, Zito G, et al. Is the Complement Protein C1q a Pro- or Anti-tumorigenic Factor? Bioinformatics Analysis Involving Human Carcinomas. Frontiers in immunology 2019;10:865 [PubMed: 31130944]

Significance:

Findings illuminate a novel direction for developing effective treatment of irreversible dry mouth, which is common after radiotherapy for head-and-neck cancer and for which no effective treatments are available.

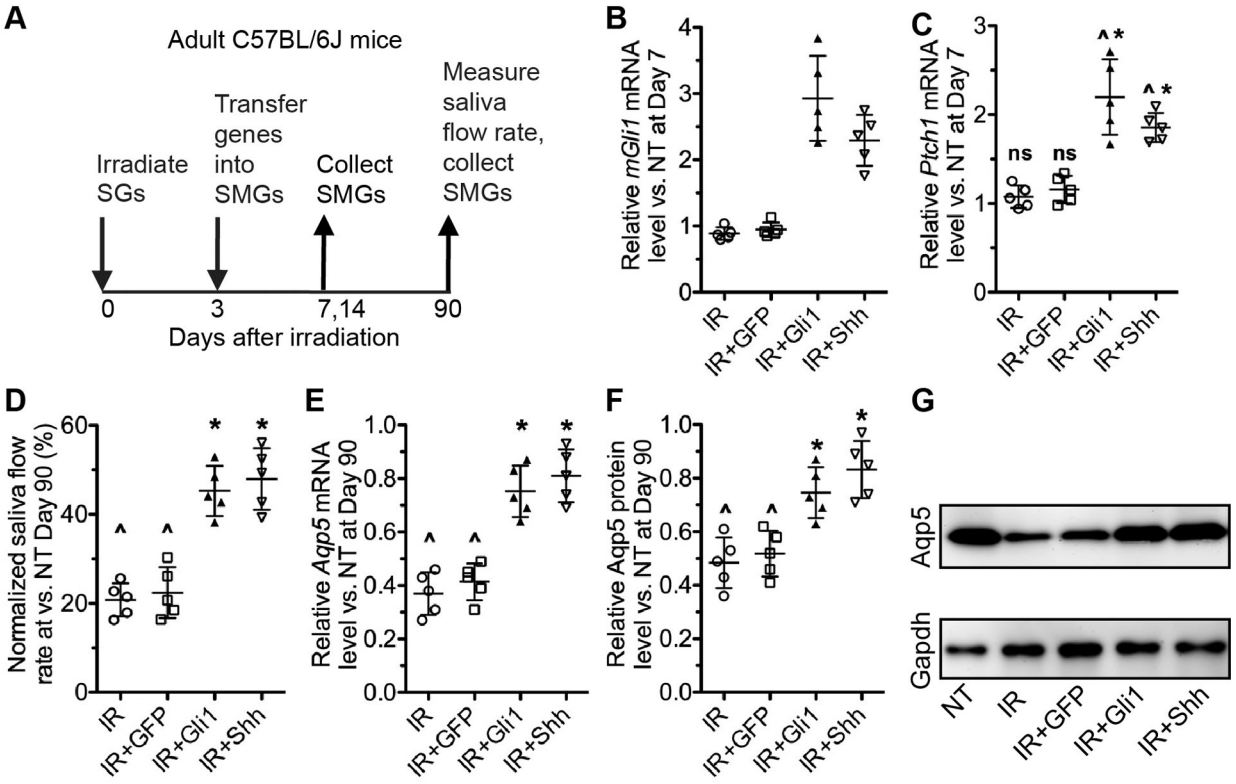

Figure 1. Effects of transient activation of Hedgehog-Gli signaling after IR on salivary function.

A: The experiment design.

B-C: The expression of Hedgehog target genes in mouse SMGs collected 7 days after IR was examined by qRT-PCR. NT: not treated.

D: The pilocarpine-stimulated whole saliva flow rates were measured at Day 90 after IR and normalized to that in NT group.

E: The mRNA level of Aqp5 in mouse SMGs collected 90 days after IR was examined by qRT-PCR.

F-G: The protein level of Aqp5 in mouse SMGs collected 90 days after IR was examined by western blot and normalized to corresponding Gapdh levels.

All quantified data were presented as Mean±SD. N = 5, ns: not significant ($P > 0.05$) vs. NT, ^: $P < 0.05$ vs. NT, *: $P < 0.05$ vs. IR and IR+Ad-GFP.

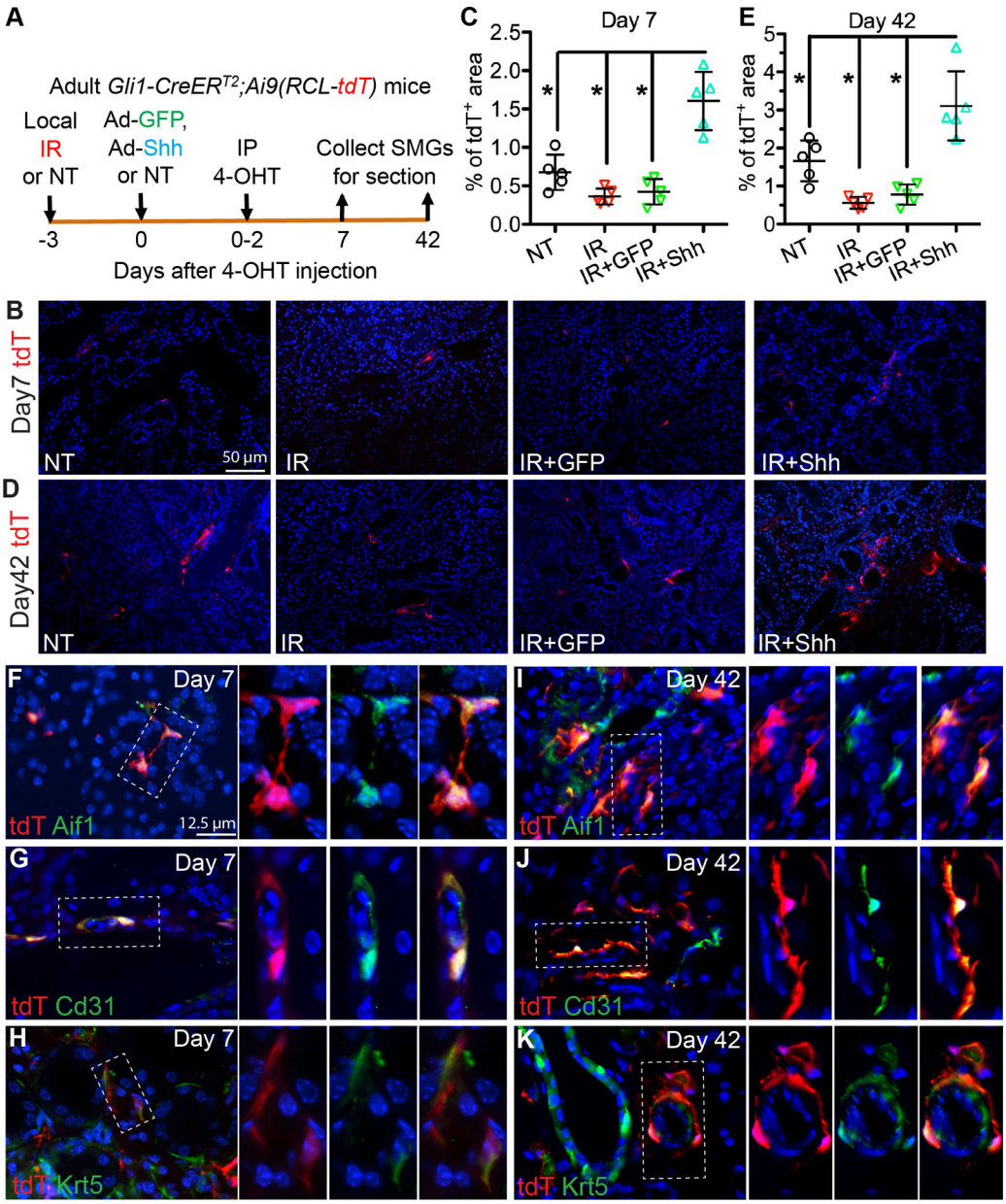

Figure 2. Lineage tracing of Gli1$^+$ cells in SMGs.

A: Experiment design. SMGs were not treated (NT), irradiated (IR), or treated with Ad-GFP or Ad-Shh after IR, and then Gli1$^+$ cells were labeled by 4-OHT IP injection.

B-E: In SMGs collected at 7 or 42 days after 4-OHT induction, tdT$^+$ cells in sections were imaged, and percentages of tdT$^+$ areas in each 200x field were quantified from 15 fields of 5 independent samples for each group. *: $P < 0.05$.

F-K: IF was performed on frozen sections of day 7 and 42 SMGs to determine the expression of markers for macrophage (Aif1), endothelia (Cd31), and basal/myo-epithelia (Krt5) in tdT$^+$ cells. Dashed boxes are enlarged to show images of tdT signal, marker signal, and merged signals of same fields respectively.

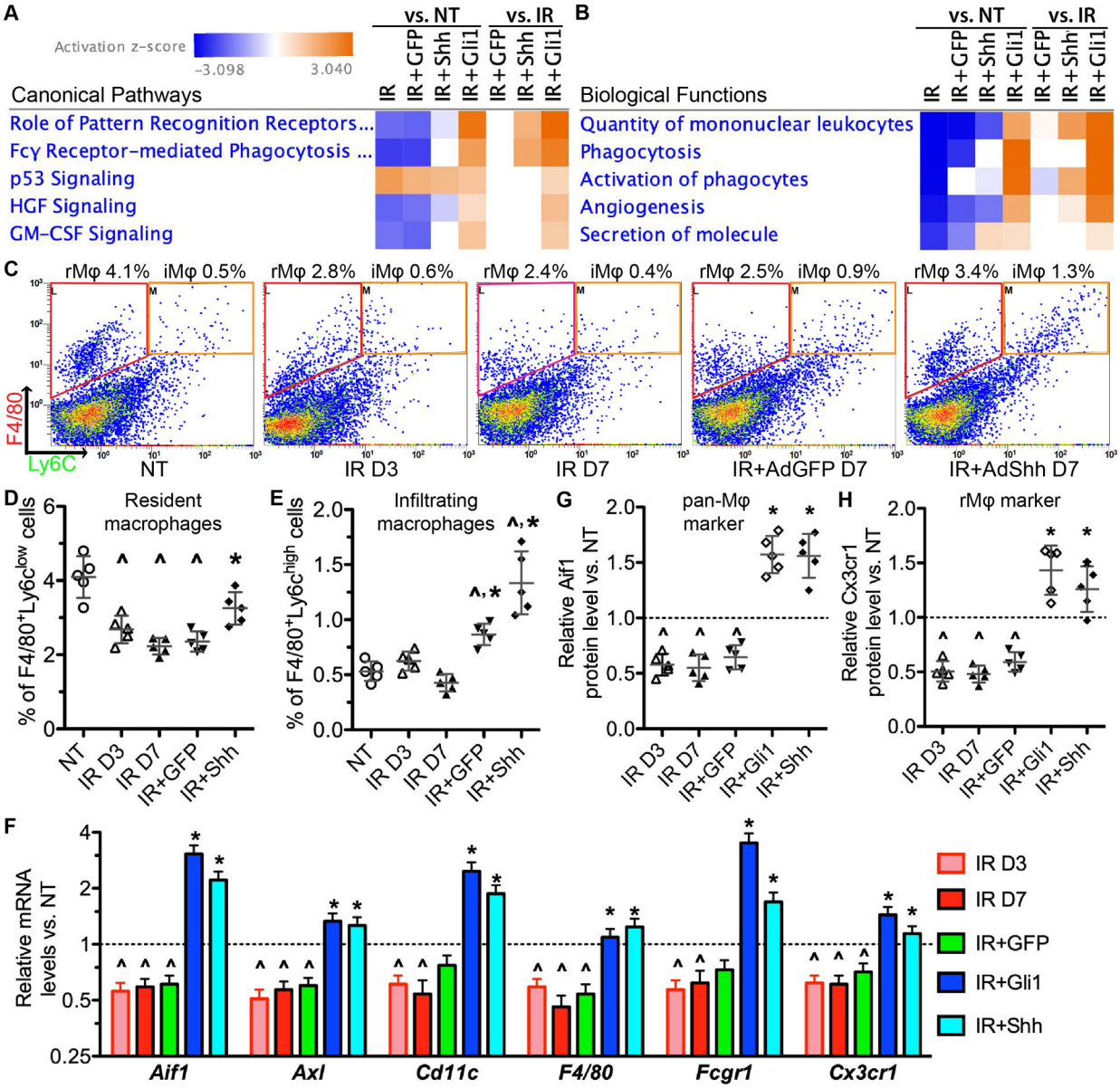

Figure 3. Effects of IR and Hedgehog activation on SMG macrophages.

A-B: IPA of RNA-seq data related to macrophages. Z-scores were shown in the heat maps. Z-scores ≥2 or ≤−2 are considered as significantly activated or inhibited respectively. N = 3.

C-E: Flow cytometric analyses on F4/80^{+}/Ly6c^{low} SG-resident macrophages (rMϕ) and F4/80^{+}/Ly6c^{high} infiltrating macrophages (iMϕ) (C) and the related quantification data (D-E). D3: day 3; D7: day 7.

F: qRT-PCR assay on mRNA expression of pan-macrophage markers (Aif1, Axl, Cd11c, F4/80, Fcgr1) and rMϕ marker Cx3cr1 in SMGs.

G-H: ELISA on protein expression of pan-macrophage marker Aif1 and rMϕ marker Cx3cr1 in the lysate of SMGs.

N = 5 in C-H, ^: P < 0.05 vs. NT; *: P < 0.05 vs. IR D7.

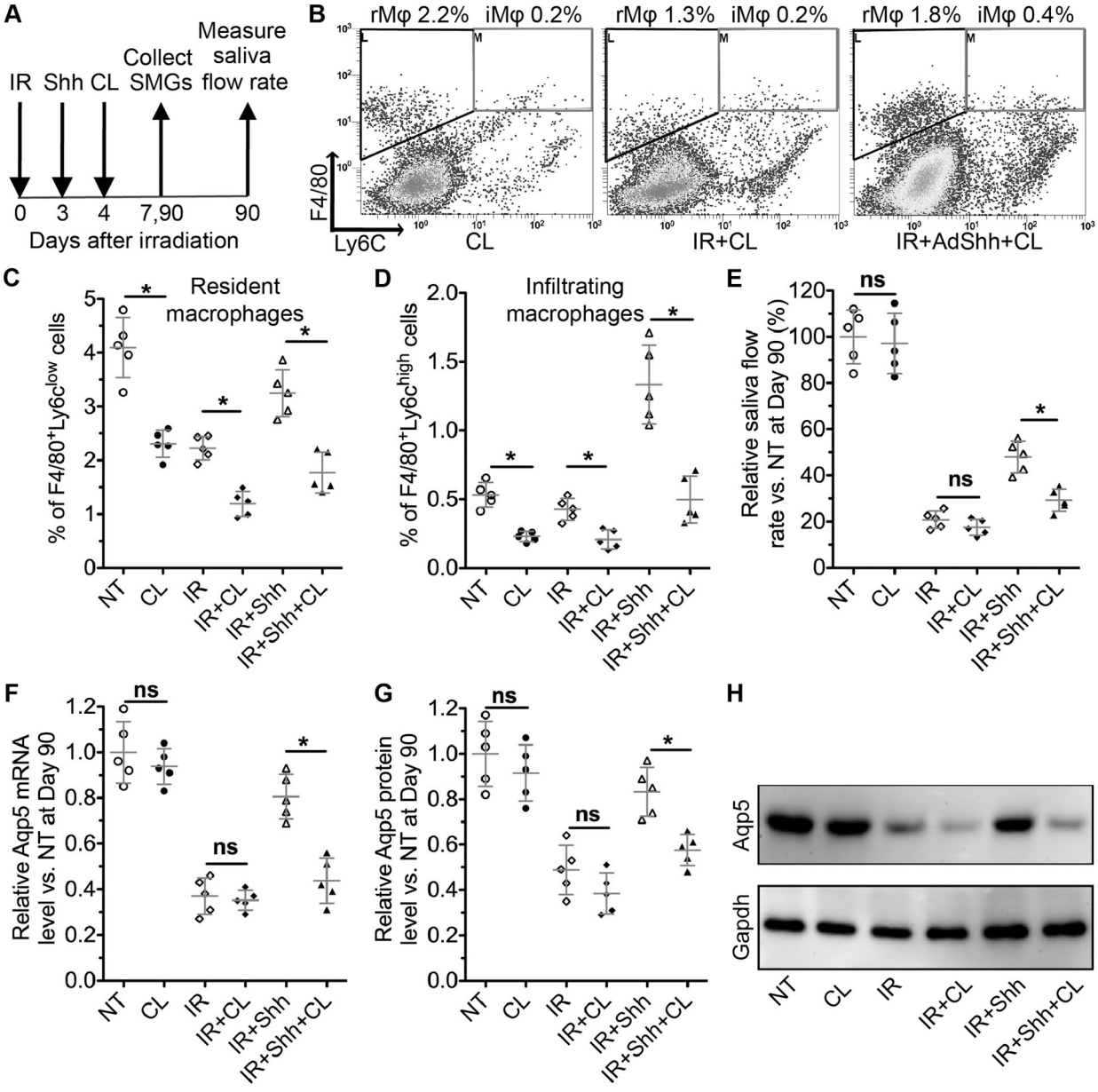

Figure 4. Effects of depleting SMG macrophages on Hedgehog-mediated rescue of IR-impaired salivary function.

A: The experiment design.

B-D: SMGs were collected 7 days after IR or 3 days after CL treatment, and analyzed with flow cytometric for $F4/80^{+}/Ly6c^{low}$ SG-resident macrophages and $F4/80^{+}/Ly6c^{high}$ infiltrating macrophages.

E: The pilocarpine-stimulated whole saliva flow rates were measured at Day 90 after IR and normalized to that in NT group.

F: The mRNA level of Aqp5 in mouse SMGs collected 90 days after IR was examined by qRT-PCR.

G: The protein level of Aqp5 in mouse SMGs collected 90 days after IR was examined by western blot and normalized with corresponding Gapdh levels.

N = 5, *: P < 0.05, ns: not significant.

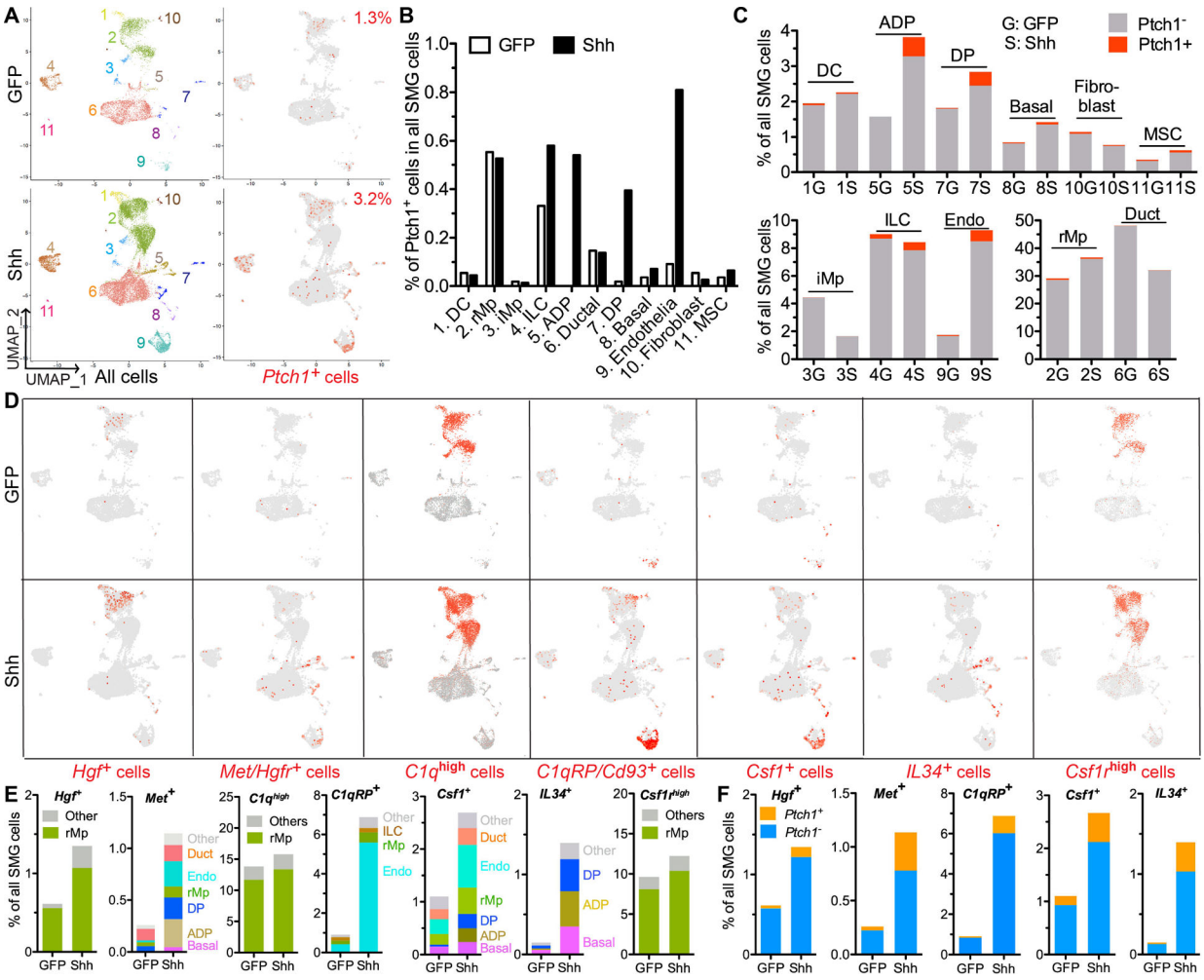

Figure 5. Single cell RNA-seq analyses on effects of Hedgehog activation on major types of SMG cells and their paracrine interactions.

A-C: At 7 days after intra-SMG transfer of GFP or Shh gene, SMG cells were analzyed with sc RNA-seq to explore the identities and percentages of all major types of SMG cells and *Ptch1*$^{+}$ Hedgehog-responsive cells based on the expression of corresponding marker genes. The putative identities of clusters are 1) DC: dendritic cells, 2) rMp: resident macrophages, 3) iMp: infiltrating macrophages, 4) ILCs: innate lymphoid cells, 5) ADP: acinar/ductal progenitors, 6) ductal cells, 7) DP: ductal progenitors, 8) Basal: basal/myo-epithelial cells, 9) Endothelia, 10) Fibroblasts, 11) MSC: mesenchymal stem cells.

D-E: In these cell clusters, cells were labeled red for all detectable expression of *Hgf, Met/Hgfr, Cd93, Csf1 or IL34* and for high expression (>50th percentile) of all *C1q* genes (*C1qa, C1qb, C1qc*) or *Csf1r* (D). Cells positive for these genes in each cell clusters were quantified as percentages of all SMG cells (E).

F. In cells expressing the above genes except *C1q* and *Csf1r*, *Ptch1*$^{+}$ and *Ptch1*$^{-}$ cells were quantified as percentages of all SMG cells.

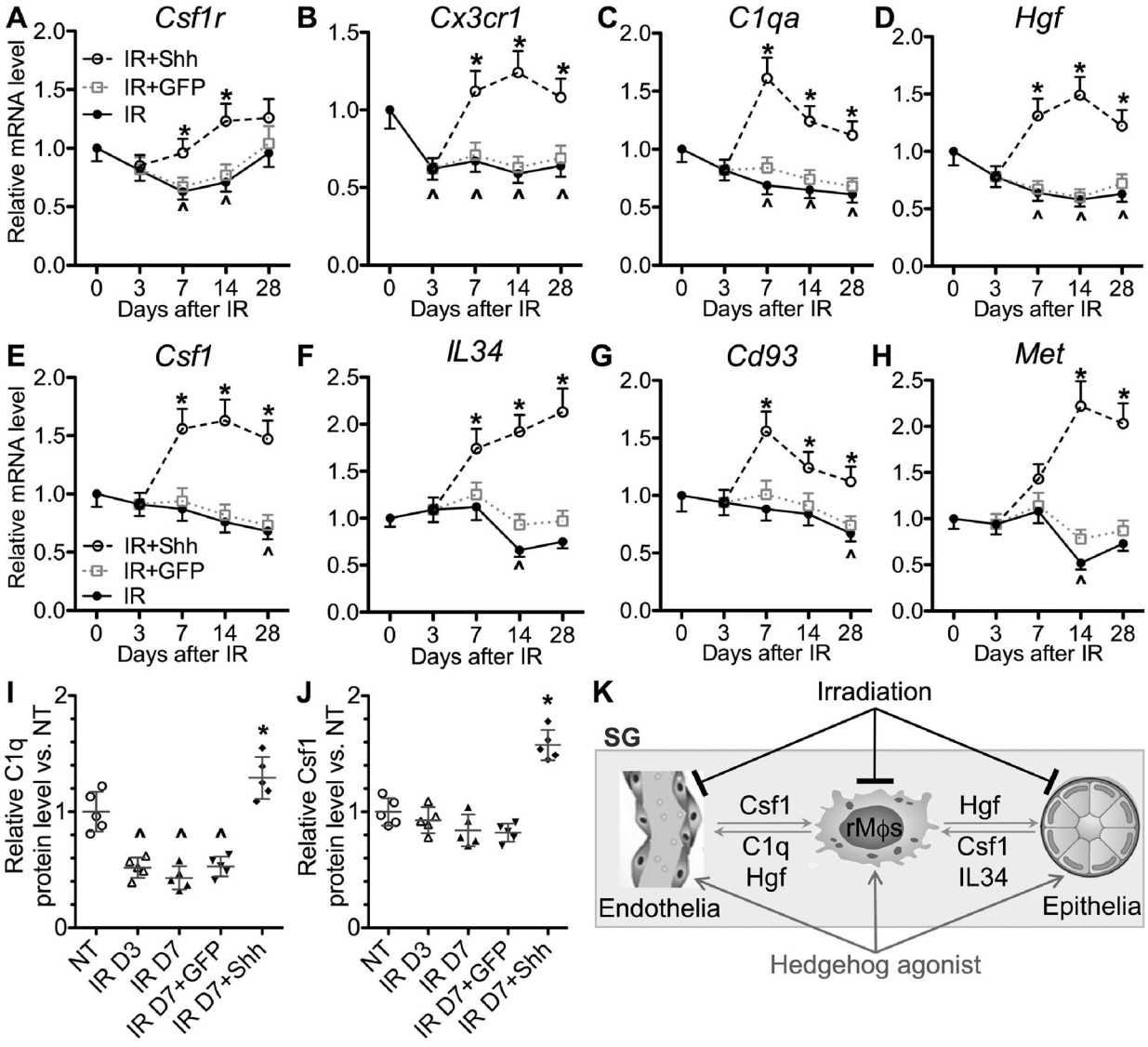

Figure 6. Effects of IR and tranisent Hedgehog activation after IR on the expression of genes in Csf1r, C1q and Hgf signaling pathways.

A-H: SMGs were collected at 3, 7, 14 and 28 days after IR with or without intra-SMG transfer of GFP or Shh gene at day 3. The mRNA levels of Csf1r, Cx3cr1, C1qa, Hgf, Csf1, IL34, Cd93, and Met were examined by qRT-PCR and normalized to non-treated (NT) samples at corresponding time points.

I-J: The levels of C1q and Csf1 proteins in the lysate of SMGs at 3 and 7 days after IR with or without intra-SMG transfer of GFP or Shh gene at day 3 were examined with ELISA and normalized to those in NT SMGs.

N = 5. *: $P < 0.05$ vs. IR D7, ^: $P < 0.05$ vs. NT.

K: Scheme of paracrine interactions between SG-resident macrophages (rMϕs), epithelial progenitors and endothelial cells, and effects of IR and Hedgehog activation on these interactions. In healthy SGs, resident macrophages secret Hgf and C1q to facilitate the maintenance of Met^+ epithelial progenitors and $Cd93^+$ and/or Met^+ endothelial cells; conversely, epithelial progenitors and endothelial cells secret Csf1 and IL34 to maintain

Csf1r^{high} resident macrophages. IR rapidly decreases the quantity of SG-resident macrophages and the levels of Hgf and C1q, which consequently impairs the recovery of epithelial progenitors and endothelial cells from IR damage, and decreases the levels of Csf1 and IL34 relatively later. Transient Hedgehog activation shortly after IR reverses the decrease of SG-resident macrophages and their paracrine interactions with epithelial progenitors and endothelial cells, which is essential for rescuing the IR-impaired salivary function.